Drilling dynamics under 1:1 internal resonance between axial and torsional modes

Sunit K Gupta* and Pankaj Wahi*
* *Department of Mechanical Engineering, Indian Institute of Technology Kanpur, India*

Summary. In the current work, we investigate the nonlinear dynamics of a lumped parameter model of rotary drilling under 1:1 internal resonance between the axial and torsional modes using the method of multiple scales. We observe that there is a transition in the nature of the Hopf-bifurcation from super-critical to sub-critical after a critical operating point.

Introduction

Bifurcation characteristic in the state-dependent delay model for regenerative machine tool vibration are generally found to be sub-critical in nature [1, 2]. However, Gupta and Wahi [3] using a global model for rotary drilling (which for small amplitude motions is equivalent to the state-dependent delay model of drilling [4]) observed super-critical Hopf-bifurcations. On exploring the dynamics of rotary drilling using this global model for the case of $1:1$ internal resonance between the axial and torsional modes, we have numerically observed a transition from super-critical to sub-critical bifurcations as the rotary speed is decreased. In the current work, we investigate this transition analytically using the method of multiple scales.

Mathematical model of regenerative drilling and its analysis

The non-dimensionalized 2-DOF model for regenerative drilling process, in the absence of any self-interruption (bit-bounce or stick-slip), is a state-dependent delayed differential equation of the form [3, 4]

$$\ddot{x}(\tau) + 2\zeta\beta\dot{x}(\tau) + \beta^2 x(\tau) = n\psi\delta_0 - n\psi\left(x(\tau) - x(\tau-\tau_n) + v_0\tau_n\right), \tag{1a}$$

$$\ddot{\theta}(\tau) + 2\kappa\dot{\theta}(\tau) + \theta(\tau) = n\delta_0 - n\left(x(\tau) - x(\tau-\tau_n) + v_0\tau_n\right), \tag{1b}$$

where ζ and κ represent the axial and torsional damping factors, respectively, β represents the natural frequency ratio between the axial and torsional modes, ψ represents the non-dimensional cutting coefficient, $\delta_0\ (= 2\pi v/n)$ is the non-dimensional steady depth of cut per cutter with $v = \dfrac{v_0}{\omega_0} = \dfrac{n\delta_0}{2\pi}$ as the non-dimensional velocity ratio. The time delay (τ_n) in Eq. (1) is determined by $\tau_n = \tau_0 - \dfrac{\theta(\tau) - \theta(\tau-\tau_n)}{\omega_0}$ with τ_0 as the constant delay or the time period for one revolution $(\dfrac{2\pi}{n\omega_0})$. It can be noted from Eq. (1) that the substitution of $\beta = 1$, $\theta = \dfrac{x}{\psi}$ and $\zeta = \kappa$ reduces the above 2-DOF system to a single degree of freedom system in only x as

$$\ddot{x}(\tau) + 2\kappa\dot{x}(\tau) + x(\tau) = 2\pi v\psi - n\psi(x(\tau) - x(\tau-\tau_n) + v\omega_0\tau_n), \tag{2}$$

and the equation governing the delay becomes $\quad \tau_n = \tau_0 - \dfrac{(x(\tau) - x(\tau-\tau_n))}{\omega_0\psi}.$ (3)

The steady state solution of Eqs. (2) and (3) is given by $x_s = 0$ and $\tau_s = \tau_0$. For small disturbances, we substitute $x(\tau) = \epsilon\eta(\tau)$ with $\eta(\tau) \ll 1$ in Eq. (3) and solve for the delay τ_n explicitly in terms of a series in ϵ as

$$\begin{aligned}\tau_n = \tau_0 &+ \epsilon\frac{1}{\omega_0\psi}\left(\eta(\tau-\tau_0) - \eta(\tau)\right) - \epsilon^2\left(\frac{1}{\omega_0\psi}\right)^2 \dot{\eta}\left(\tau-\tau_0\right)\left(\eta(\tau-\tau_0) - \eta(\tau)\right) \\ &+ \epsilon^3\left(\frac{1}{\omega_0\psi}\right)^3\left(\dot{\eta}(\tau-\tau_0)^2\left(\eta(\tau-\tau_0) - \eta(\tau)\right) + \frac{\ddot{\eta}\left(\tau-\tau_0\right)}{2}\left(\eta(\tau-\tau_0) - \eta(\tau)\right)^2\right).\end{aligned} \tag{4}$$

Now, on substituting τ_n from Eq. (4) and $x(\tau) = \epsilon\eta(\tau)$ in Eq. (2) and expanding in a Taylor series while retaining terms till $\mathcal{O}(\epsilon^3)$, we get

$$\begin{aligned}&\epsilon\left(\ddot{\eta} + 2\,\kappa\dot{\eta} + \eta + n\psi\left(\eta - \eta_{\tau 0}\right)\left(1 - \frac{v}{\psi}\right)\right) + \epsilon^2\left(n\psi\dot{\eta}_{\tau 0}\left(\eta - \eta_{\tau 0}\right)\left(\frac{v-\psi}{\omega_0\psi^2}\right)\right) \\ &- \epsilon^3\left(\frac{n\psi}{2}\left(\eta - \eta_{\tau 0}\right)\left(\ddot{\eta}_{\tau 0}\eta_{\tau 0} - \eta\ddot{\eta}_{\tau 0} + 2\dot{\eta}_{\tau 0}^2\right)\right)\left(\frac{v-\psi}{\omega_0^2\psi^3}\right) = 0\end{aligned} \tag{5}$$

with $\eta_{\tau 0} = \eta(\tau - \tau_0)$. Note that the above DDE (Eq. (5)) now involves delayed terms with a constant delay only. It can be observed that the $\mathcal{O}(\epsilon)$ term in Eq. (5) gives the linearized equation about the steady state. A linear stability analysis in the parametric space of $\omega_0 - v$ reveals the Hopf-bifurcation point as

$$\omega_{0,cr} = \frac{2\,\pi\,\omega}{n\left(2\,\pi + \arctan\left(-4\,\frac{\omega\,\kappa\,(\omega^2-1)}{\omega^4-2\,\omega^2+1+4\,\omega^2\kappa^2}, \frac{-\omega^4-1+4\,\omega^2\kappa^2+2\,\omega^2}{\omega^4-2\,\omega^2+1+4\,\omega^2\kappa^2}\right)\right)}, \tag{6}$$

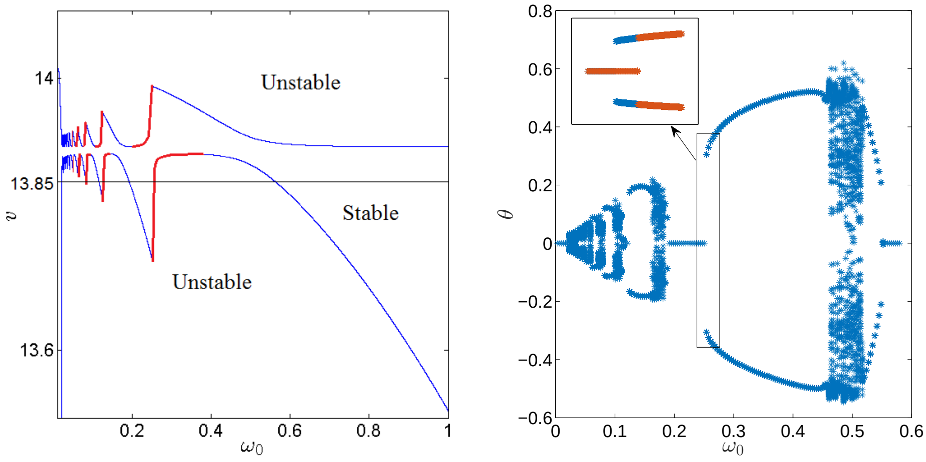

(i) (ii)

Figure 1: (i) Stability boundary with $n = 4$, $\psi = 13.8943$, $\beta = 1$ and $\kappa = 0.01$ depicting sub- and super- critical Hopf bifurcation marked using Red and Blue color, respectively. (ii) Bifurcation diagram with varying ω_0 representing the θ values corresponding to $\dot{x} = 0$ for $v = 13.85$.

$$v_{cr} = \frac{1}{2}\frac{\omega^4 - 2\,\omega^2 n\psi - 2\,\omega^2 + 2\,n\psi + 1 + 4\,\omega^2\kappa^2}{n\,(1-\omega^2)}\,, \tag{7}$$

where ω is the frequency of the ensuing limit cycles from the Hopf-bifurcation point. In order to analyze the nonlinear dynamics of the system close to the Hopf point, we perturb one of the operating parameters, viz. $\omega_0 = \omega_{0,cr} - \epsilon^2 k_1$ with $k_1 > 0$ in Eq. (5). We next introduce multiple time scales as $T_0 = \tau$, $T_1 = \epsilon\tau$, $T_2 = \epsilon^2\tau$ and follow the procedure described in [2, 5]. The final slow flow equation governing the evolution of the amplitude R is

$$\dot{R} = \epsilon^2 \frac{-4\,n\omega^2\psi^2\omega_{0,cr}\pi\,p_1\,p_2\,q_1\,k_1\,R + n\omega^4\left(2\kappa\,n\,p_1^2\,q_2\omega_{0,cr} + 384\pi\,p_1\omega^4\kappa^6 - 48\omega^2\,q_2\,p_1^3\,\kappa^4 - 4\,q_4\,p_1^4\kappa^2 - 3\,q_3\,p_1^6\right)R^3}{2\psi^2\left(4n^2p_1^2\,p_3\,p_2\,\omega_{0,cr}^3 + 4\kappa\pi\,n\,p_1\,p_4\,p_2\,\omega_{0,cr}^2 + \pi^2\left(p_1^2 + 4\omega^2\kappa^2\right)p_2\omega_{0,cr}\right)} \tag{8}$$

where $p_1 = (\omega^2 - 1)$, $p_2 = 36\omega^2\kappa^2 + 16\omega^8 - 40\omega^6 + 33\omega^4 - 10\omega^2 + 1$, $q_1 = (2\kappa)^2 - p_1^2$, $p_3 = \omega^2 + \kappa^2$, $p_4 = 3\omega^4 - 2\omega^2 + 4\omega^2\kappa^2 - 1$, $q_2 = 96\omega^2\kappa^4 - \left(48\omega^6 - 196\omega^4 + 32\omega^2 - 8\right)\kappa^2 - 36\omega^8 + 63\omega^6 - 18\omega^4 - 9\omega^2$, $q_3 = 1 - 2\omega^2$, $q_4 = 8\omega^4 - 4\omega^2 + 5$. The non-trivial solution for the amplitude of the limit cycle (R) from Eq. (8) is

$$R = \sqrt{\frac{4\,n\omega^2\psi^2\omega_{0,cr}\pi\,p_1\,p_2\,q_1\,k_1}{n\omega^4\left(2\kappa\,n\,p_1^2\,q_2\omega_{0,cr} + 384\pi\,p_1\omega^4\kappa^6 - 48\omega^2\,q_2\,p_1^3\,\kappa^4 - 4\,q_4\,p_1^4\kappa^2 - 3\,q_3\,p_1^6\right)}} \tag{9}$$

Since $-4\,n\omega^2\psi^2\omega_0\pi\,p_1\,p_2\,q_1\,k_1 > 0$, the nature of the Hopf-bifurcation is decided by the sign of the denominator of Eq. (9). Hence, the transition from super- to sub- critical bifurcation can be determined from the condition

$$2\kappa\,n\,p_1^2\,q_2\omega_{0,cr} + 384\pi\,p_1\omega^4\kappa^6 - 48\omega^2\,q_2\,p_1^3\,\kappa^4 - 4\,q_4\,p_1^4\kappa^2 - 3\,q_3\,p_1^6 = 0\,. \tag{10}$$

Substituting for $\omega_{0,cr}$ from Eq. (6), we solve the above for ω and obtain the operating parameters for transition from super- to sub- critical bifurcations from Eqs. (6) and (7). The stability curve, for $\psi = 13.8943$, $n = 4$ and $\kappa = 0.01$, depicting different regions for sub and super-critical bifurcation has been shown with different colors in Fig.1i. In Fig. 1ii, we have shown the bifurcation diagram obtained for rotary drilling using the global model [3] wherein we plot the θ values corresponding to the Poincaré section $\dot{x} = 0$ for $v = 13.85$. From Fig.1ii, we can clearly notice that the right portion of the stability boundary corresponds to a super-critical bifurcation whereas the left portion involves a sub-critical bifurcation. Hence, numerical simulations verify the analytical findings of the method of multiple scales.

Conclusion

Transition in the bifurcation characteristics in the state-dependent delay model of rotary drilling has been analyzed using the method of multiple scales. In general, a reduction in rotary speed leads to a subcritical bifurcation.

References

[1] Kalmár-Nagy T., Stépán G., Moon F.C. (2001) Subcritical Hopf bifurcation in the delay equation model for machine tool vibrations. *Nonlin Dyn* **26**:121-142.

[2] Wahi P., Chatterjee A. (2005) Regenerative tool chatter near a codimension 2 Hopf point using the multiple scales. *Nonline Dyn* **47**:275-283.

[3] Gupta, S. K., Wahi, P. (2016) Global axial–torsional dynamics during rotary drilling. *J. Sound Vib* **375**:332-352.

[4] Nandakumar K., Wiercigroch M. (2013) Stability analysis of a state dependent delayed, coupled two DOF model of drill-string vibration. *J. Sound Vib* **332**:2575 - 2592.

[5] Das S.L., Chatterjee A. (2002) Multiple scales without center manifold reductions for delay differential equations near Hopf bifurcation. *Nonline Dyn* **30**:323-335.